Progress In Electromagnetics Research, PIER 91, 319–332, 2009

MODIFIED PLANE WAVE METHOD ANALYSIS OF DIELECTRIC PLASMA PHOTONIC CRYSTAL

L. Qi and Z. Yang

Institute of High Energy Electronics
University of Electronic Science and Technology of China
No. 4, Section 2, North Jianshe Road, Chengdu 610054, P. R. China

Abstract—Dispersion characteristics of two types of two-dimension dielectric plasma photonic crystal are studied based on modified plane wave method. Firstly, the eigenvalue equations of TM mode of type-1 and type-2 structures are derived respectively; their dispersion curves are confirmed by the software simulation. Secondly, the influences of normalized plasma frequency, filling factor and relative dielectric constant on photonic band gap, and relative photonic band gap width are analyzed respectively, and some corresponding physical explanations are also given. These results would provide theoretical instructions for designing new photonic crystal devices using plasma-dielectric structure.

1. INTRODUCTION

Photonic crystal (PC) has attracted much attention since the initial predictions of Yablonovitch and John [1–7]. This active research area has been extended to plasma PC which is expected to obtain more particular characteristics than the conventional one [8–15]. It is well known that electromagnetic waves with frequency below plasma frequency cannot propagate through a bulk plasma; if dielectric components are introduced periodically, it is possible for electromagnetic waves to be guided below the plasma frequency, and photonic band gaps (PBG) can be formed attributing to the surface plasma polarization.

One-dimension (1D) unmagnetized plasma PC is an artificially periodic array composed of alternating plasma and dielectric. Hojo et al. proposed the conception of plasma PC and studied the dispersion

Corresponding author: L. Qi (qilimei1204@163.com).

relation of electromagnetic waves in 1D plasma PC using transfer matrix method (TMM) [8]. Liu et al. discussed the influence of plasma parameters on transmission and reflection coefficients for 1D plasma PC using finite-difference time-domain (FDTD) method [9]. In recent years, two-dimension (2D) unmagnetized plasma PC has been attached more importance for their potential controlling devices of millimeter waves [10–15]. There are two types of 2D plasma PC [15]. The first type (type-1) is a 2D PC in which plasma rods are arranged in dielectric periodically, while the second one (type-2) is an antiparallel structure composed of dielectric in a plasma bulk. However, for the two types of PC, researches mentioned above are mainly on plasma arrays in air or air holes in plasma.

In this paper, using modified plane wave method (PWM), we derive the eigenequations of TM mode of type-1 and type-2 plasma PC when the dielectric is not mere an air. The validity of the eigenequations is confirmed by CST MICROWAVE STUDIO. Moreover, we investigate the influence of normalized plasma frequency, filling factor and relative dielectric constant on PBG and relative PBG width, and give some corresponding physical explanations respectively.

2. THEORETICAL MODEL AND MODIFIED PLANE WAVE METHOD

Figures 1(a) and 1(b) show the schematic structures of two types of 2D plasma PC with square lattice. We assume the radius of the circular rods and lattice constant are R and a respectively; the relative dielectric function for circular rods and background are ε_a

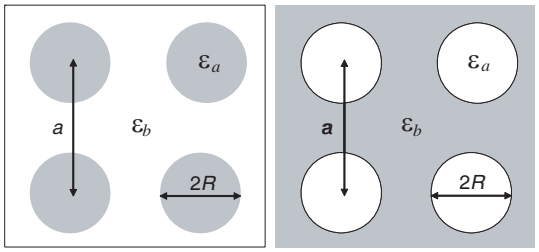

Figure 1. Schematic structures of 2-D square lattice plasma PC. (a) type-1 with circular plasma rods immersed in dielectric background and (b) type-2 with circular dielectric rods in bulk plasma. The gray area represents plasma.

and ε_b, respectively. In this paper, we utilize the frequency-dependent dielectric function for the unmagnetized collisionless plasma that meets the Drude formula [8, 16]:

$$\varepsilon(\omega) = 1 - \frac{\omega_p^2}{\omega^2} \tag{1}$$

where ω is the electromagnetic wave frequency and $\omega_p = (e^2 n_p/\varepsilon_0 m)^{1/2}$ is the electron plasma frequency with an electron density n_p. In terms of the plasma PC, the dielectric function of plasma is usually dependent on electromagnetic wave frequency and less than 1; if we control electron plasma frequency by changing electron density, the PBG is controllable; this phenomena has not been realized in conventional PC.

Many theoretical and numerical tools have been developed to calculate the dispersion curves of photonic crystals, such as plane wave method (PWM) [11, 13, 17], finite-difference time-domain (FDTD) method [9, 11, 18], transfer-matrix method [8, 19, 20], multiple multipole method [21], and nonperturbative approach [22]. Among these methods, PWM is the most popular technique. In this article, we will modify the PWM eigenequation to a standard one that is capable of analyzing the dielectric plasma photonic crystals.

The conventional eigenvalue equation for TM mode in PC can be written as [17]:

$$\begin{aligned} \left|\mathbf{k}_{//}+\mathbf{G}_{//}\right|^2 \mathbf{B}(\mathbf{k}_{//},\mathbf{G}_{//}) &= \frac{\omega^2}{c^2}\sum_{\mathbf{G}'_{//}} \hat{\varepsilon}(\mathbf{G}_{//}-\mathbf{G}'_{//})\mathbf{B}(\mathbf{k}_{//},\mathbf{G}'_{//}) \\ = \frac{\omega^2}{c^2}\hat{\varepsilon}(0)\mathbf{B}(\mathbf{k}_{//},\mathbf{G}_{//}) &+ \frac{\omega^2}{c^2}\sum_{\mathbf{G}'_{//}\neq\mathbf{G}_{//}} \hat{\varepsilon}(\mathbf{G}_{//}-\mathbf{G}'_{//})\mathbf{B}(\mathbf{k}_{//},\mathbf{G}'_{//}) \end{aligned} \tag{2}$$

where ω is wave frequency; c is the speed of light in vacuum; $\mathbf{k}_{//}$ is wave vector. $\mathbf{B}(\mathbf{k}_{//},\mathbf{G}_{//})$ and $\hat{\varepsilon}(\mathbf{G})$ is the Fourier coefficient of electric field and position-dependent dielectric constant, respectively.

2.1. Type 1

For type-1 plasma PC the Fourier coefficient of $\hat{\varepsilon}(\mathbf{G})$ can be written as:

$$\hat{\varepsilon}(\mathbf{G}_{//}) = \begin{cases} \varepsilon_b + \left(1 - \dfrac{\omega_p^2}{\omega^2} - \varepsilon_b\right) f & \mathbf{G}_{//} = 0 \\ \left(1 - \dfrac{\omega_p^2}{\omega^2} - \varepsilon_b\right) f \dfrac{2J_1(|\mathbf{G}_{//}|R)}{|\mathbf{G}_{//}|R} & \mathbf{G}_{//} \neq 0 \end{cases} \tag{3}$$

If Eq. (3) is substituted into Eq. (2) to make the transposition, the eigenvalue equation of TM mode can be obtained:

$$\sum_{\mathbf{G}'_{//}}\left[\left|\mathbf{k}_{//}+\mathbf{G}_{//}\right|^2\delta_{\mathbf{G}_{//},\mathbf{G}'_{//}}+f\frac{\omega_p^2}{c^2}\frac{2J_1\left(\left|\mathbf{G}_{//}-\mathbf{G}'_{//}\right|R\right)}{\left(\left|\mathbf{G}_{//}-\mathbf{G}'_{//}\right|R\right)}\right]\mathbf{B}(\mathbf{k}_{//},\mathbf{G}'_{//})$$
$$=\frac{\omega^2}{c^2}\sum_{\mathbf{G}'_{//}}\left[\varepsilon_b\delta_{\mathbf{G}_{//},\mathbf{G}'_{//}}+(1-\varepsilon_b)f\frac{2J_1\left(\left|\mathbf{G}_{//}-\mathbf{G}'_{//}\right|R\right)}{\left(\left|\mathbf{G}_{//}-\mathbf{G}'_{//}\right|R\right)}\right]\mathbf{B}(\mathbf{k}_{//},\mathbf{G}'_{//}) \quad (4)$$

Eq. (4) can be rewritten as:

$$\left[(\mathbf{I}+\mathbf{N})^{-1}\mathbf{M}-\frac{\omega^2}{c^2}\right]\mathbf{B}=\mathbf{0} \quad (5)$$

Therefore, the dispersion characteristic for type-1 plasma PC can be achieved by solving the standard eigenvalue problem for a real, symmetric matrix. The elements of matrices $\mathbf{M}$, $\mathbf{N}$, $\mathbf{I}$ are defined by

$$\begin{aligned}M&=\frac{\left|\mathbf{k}_{//}+\mathbf{G}_{//}\right|^2}{\varepsilon_b}\delta_{\mathbf{G}_{//},\mathbf{G}'_{//}}+\frac{\omega_p^2}{c^2\varepsilon_b}f\frac{2J_1\left(\left|\mathbf{G}_{//}-\mathbf{G}'_{//}\right|R\right)}{\left(\left|\mathbf{G}_{//}-\mathbf{G}'_{//}\right|R\right)}\\ N&=\frac{(1-\varepsilon_b)}{\varepsilon_b}f\frac{2J_1\left(\left|\mathbf{G}_{//}-\mathbf{G}'_{//}\right|R\right)}{\left(\left|\mathbf{G}_{//}-\mathbf{G}'_{//}\right|R\right)}\\ I&=\delta_{\mathbf{G}_{//},\mathbf{G}'_{//}}\end{aligned} \quad (6)$$

2.2. Type-2

For type-2 structure, the Fourier coefficient of $\hat{\varepsilon}(\mathbf{G})$ can be written as:

$$\hat{\varepsilon}(\mathbf{G}_{//})=\begin{cases}1-\dfrac{\omega_p^2}{\omega^2}+\left(\varepsilon_a-1+\dfrac{\omega_p^2}{\omega^2}\right)f & \mathbf{G}_{//}=0\\ \left(\varepsilon_a-1+\dfrac{\omega_p^2}{\omega^2}\right)f\dfrac{2J_1(|\mathbf{G}_{//}|R)}{|\mathbf{G}_{//}|R} & \mathbf{G}_{//}\neq 0\end{cases} \quad (7)$$

If Eq. (7) is substituted into Eq. (2) to make the transposition, the eigenvalue of the TM mode can be written as:

$$\sum_{\mathbf{G}'_{//}}\left\{\left|\mathbf{k}_{//}+\mathbf{G}_{//}\right|^2\delta_{\mathbf{G}_{//},\mathbf{G}'_{//}}+\frac{\omega_p^2}{c^2}\left[\delta_{\mathbf{G}_{//},\mathbf{G}'_{//}}-f\frac{2J_1\left(\left|\mathbf{G}_{//}-\mathbf{G}'_{//}\right|R\right)}{\left(\left|\mathbf{G}_{//}-\mathbf{G}'_{//}\right|R\right)}\right]\right\}\mathbf{B}(\mathbf{k}_{//},\mathbf{G}'_{//})$$
$$=\frac{\omega^2}{c^2}\sum_{\mathbf{G}'_{//}}\left\{\delta_{\mathbf{G}_{//},\mathbf{G}'_{//}}+(\varepsilon_a-1)f\frac{2J_1\left(\left|\mathbf{G}_{//}-\mathbf{G}'_{//}\right|R\right)}{\left(\left|\mathbf{G}_{//}-\mathbf{G}'_{//}\right|R\right)}\right\}\mathbf{B}(\mathbf{k}_{//},\mathbf{G}'_{//}) \tag{8}$$

Equation (8) can also be written as a standard eigenvalue equation:

$$\left[(\mathbf{I}+\mathbf{N})^{-1}\mathbf{M}-\frac{\omega^2}{c^2}\right]\mathbf{B}=0 \tag{9}$$

The elements of matrices **M**, **N**, **I**

$$\begin{aligned}M&=\left|\mathbf{k}_{//}+\mathbf{G}_{//}\right|^2\delta_{\mathbf{G}_{//},\mathbf{G}'_{//}}+\frac{\omega_p^2}{c^2}\left[\delta_{\mathbf{G}_{//},\mathbf{G}'_{//}}-f\frac{2J_1\left(\left|\mathbf{G}_{//}-\mathbf{G}'_{//}\right|R\right)}{\left(\left|\mathbf{G}_{//}-\mathbf{G}'_{//}\right|R\right)}\right]\\ N&=(\varepsilon_a-1)f\frac{2J_1\left(\left|\mathbf{G}_{//}-\mathbf{G}'_{//}\right|R\right)}{\left(\left|\mathbf{G}_{//}-\mathbf{G}'_{//}\right|R\right)}\\ I&=\delta_{\mathbf{G}_{//},\mathbf{G}'_{//}}\end{aligned} \tag{10}$$

3. RESULTS AND DISCUSSIONS

Figures 2(a) and (b) show the first fifteen dispersion curves of TM mode for type-1 plasma PC with the same plasma-filling factor $f = 0.5$ and relative dielectric constant of background $\varepsilon_b = 6$, but with different normalized plasma frequency $\omega_p a/2\pi c = 0$ for Fig. 2(a) and $\omega_p a/2\pi c = 1$ for Fig. 2(b). The dispersion curves are calculated along $\Gamma(0, 0)$-$X(\pi/a, 0)$-$M(\pi/a, \pi/a)$ in the first irreducible Brillouin zone, and a total number of 441 plane waves is used. In Fig. 2(a), when Eq. (1) reduces to $\varepsilon = 1$ for $\omega_p a/2\pi c = 0$, the type-1 structure becomes a conventional dielectric PC where there is no gap for the first fifth dispersion curves. While for $\omega_p a/2\pi c = 1$ in Fig. 2(b), the type-1 plasma PC can lead to two band gaps—the larger one between the zero frequency and cut-off frequency ($TM_{0\text{-}1}$) and the smaller one between the first and the second bands ($TM_{1\text{-}2}$).

Figures 3(a) and (b) show the dispersion curves of TM mode for type-2 plasma PC with the same dielectric-filling factor $f = 0.5$ and relative dielectric constant of circular rod $\varepsilon_a = 6$, but with different normalized plasma frequency $\omega_p a/2\pi c = 0$ for Fig. 3(a) and $\omega_p a/2\pi c = 1$ for Fig. 3(b). Fig. 3(a) shows that there is a very small PBG between the third and forth bands ($TM_{3\text{-}4}$) when the background is a vacuum. If the unmagnetized plasma is introduced in the background with $\omega_p a/2\pi c = 1$, as shown in Fig. 3(b), there are five large band gaps: $TM_{1\text{-}2}$, $TM_{3\text{-}4}$, $TM_{6\text{-}7}$, $TM_{10\text{-}11}$, and $TM_{12\text{-}13}$ besides a cut-off frequency.

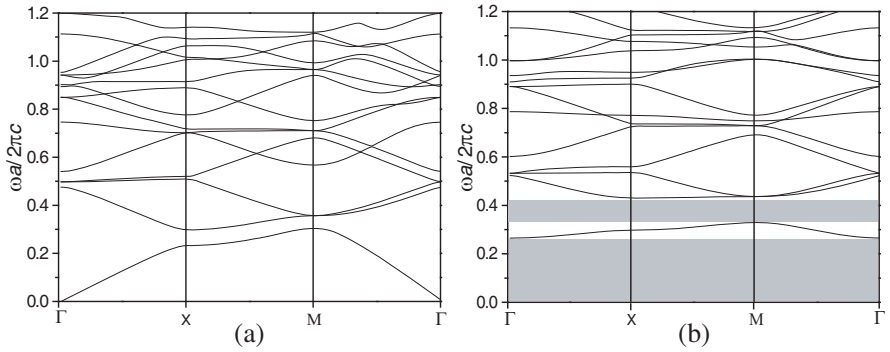

Figure 2. Dispersion curves of TM mode for type-1 plasma PC with plasma-filling factor $f = 0.5$ and relative dielectric constant of background $\varepsilon_b = 6$ but with different normalized plasma frequency. (a) $\omega_p a/2\pi c = 0$ and (b) $\omega_p a/2\pi c = 1$.

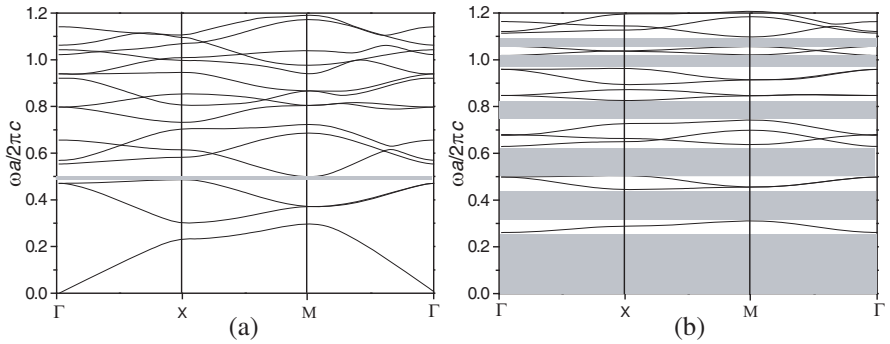

Figure 3. Dispersion curves of TM mode for type-2 plasma PC with dielectric-filling factor $f = 0.5$ and relative dielectric constant of dielectric rod $\varepsilon_a = 6$ but with different normalized plasma frequency. (a) $\omega_p a/2\pi c = 0$ and (b) $\omega_p a/2\pi c = 1$.

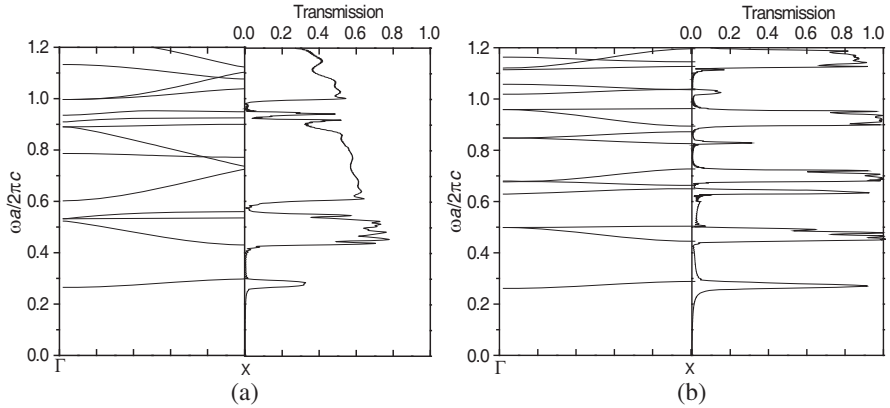

Figure 4. Transmission (curves (the right side) and the dispersion relation (the left side) of TM mode in Γ-X direction for (a) type-1 and (b) type-2 structure.

To demonstrate the results calculated above, transmissions for type-1 and type-2 DPPC are simulated using CST MICROWAVE STUDIO, a 3D EM simulation software based on Finite Integration [23]. The calculated transmission together with the dispersion relation in Γ-X direction for type-1 and type-2 plasma PC is shown in Figs. 4(a) and 4(b), respectively. Among them, plasma PC in Fig. 4(a) has the same parameters as the one in Fig. 2(b); plasma PC in Fig. 4(b) has the same parameters as that in Fig. 3(b). The left side of these figures shows the dispersion, while the right side shows the transmission; it is seen that they are basically in agreement for the two types of plasma PC.

According to the band structures above, it is found that the inclusion of plasma components in dielectric PC can bring more gaps and even enlarge the size of the gaps, and type-2 has more gaps than type-1. Therefore, these structures have potential application in PC devices when large band gap is needed. In the following section, we intend to discuss how the cutoff frequency, the 1st and 2nd edge frequencies vary with the normalized plasma frequency, filling factor and dielectric constant in detail.

3.1. Effects of Normalized Plasma Frequency on PBG

Figure 5(a) shows the variation of the cut-off frequency and edge frequencies of $TM_{1\text{-}2}$ and $TM_{3\text{-}4}$ band versus the normalized plasma frequency in type-1 plasma PC, the plasma-filling factor and relative dielectric constant of background are $f = 0.5$ and $\varepsilon_b = 6$, respectively.

One can notice that the cutoff frequency, the 1st and 2nd edge frequencies increase and tend to degenerate when the normalized plasma frequency varies from 0.2 to 2. The 1st and 2nd PBG appear at $\omega_p a/2\pi c = 0.4$ and $\omega_p a/2\pi c = 1.6$ respectively; the width of two band gaps seems to become large with normalized plasma frequency increasing. This tendency can be explained from the behavior of the relative PBG width $\Delta\omega/\omega_g$ on normalized plasma frequency in Fig. 5(b), where ω_g is the frequency at the middle gap and $\Delta\omega$ the frequency width of the gap. $\Delta\omega/\omega_g$ for $TM_{1\text{-}2}$ and $TM_{3\text{-}4}$ increase when the normalized plasma frequency increases and reach 0.03 and 0.35 at $\omega_p a/2\pi c = 2$, respectively.

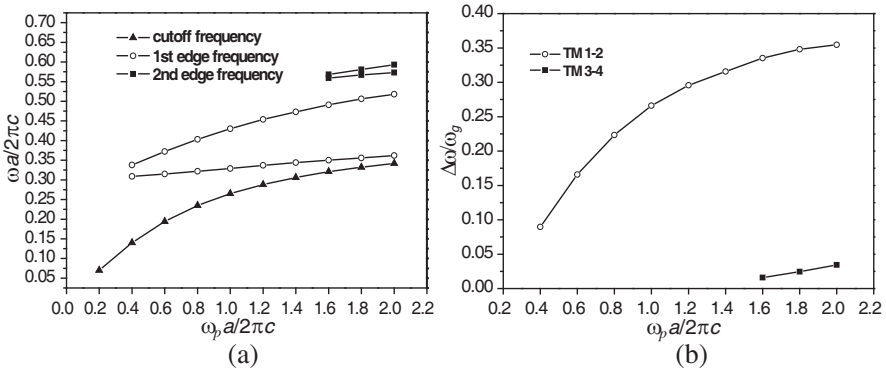

Figure 5. (a) The cutoff frequency, 1st and 2nd PBG edge frequencies, and (b) the 1st and 2nd relative PBG width versus the normalized plasma frequency for type-1 plasma PC with plasma-filling factor $f = 0.5$ and relative dielectric constant of background $\varepsilon_b = 6$.

Figure 6 shows the cut-off frequency, edge frequencies and relative PBG width as a function of normalized plasma frequency for type-2 structure, the dielectric-filling factor and relative dielectric constant of dielectric rod are $f = 0.5$ and $\varepsilon_a = 6$ respectively. Compared with type-1, the cutoff frequency, the 1st and 2nd edge frequencies shift toward higher frequency with the difference that the 1st and 2nd band gaps simultaneously emerge at $\omega_p a/2\pi c = 0.2$ and the relative PBG widths for the 1st and 2nd are larger than that of type-1. For type-2 structure, the maximum values of the 1st and 2nd relative PBG widths reach 0.28 and 0.45 respectively.

Therefore, for these two types of plasma PC, large gaps would be obtained as normalized plasma frequency increases. This can be explained by considering the skin depth in plasma. The skin depth for static modes in plasma is given by $\delta = c/\omega_p$ [11, 24], where c is

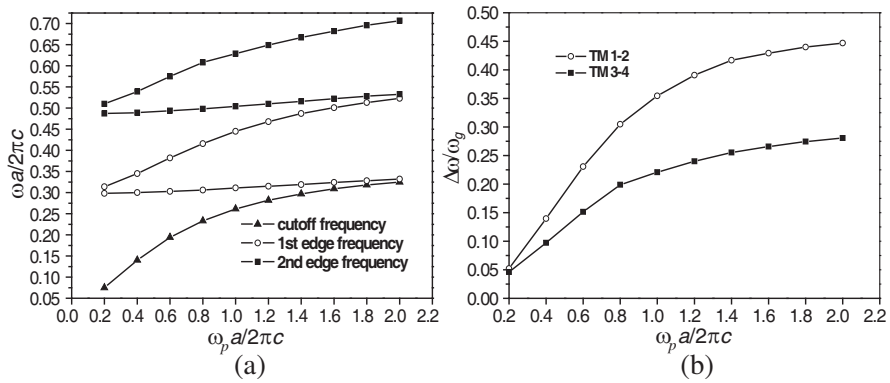

Figure 6. (a) The cutoff frequency, the 1st and 2nd edge frequencies, and (b) the 1st and 2nd relative PBG width versus the normalized plasma frequency for type-2 plasma PC with dielectric-filling factor $f = 0.5$ and relative dielectric constant of dielectric rod $\varepsilon_a = 6$.

the speed of light in vacuum. As ω_p becomes larger, the skin depth becomes smaller and the coupling between dielectric becomes weaker, then large gaps appear.

3.2. Effect of Filling Factor on PBG

Fig. 7(a) and Fig. 8(a) show the cutoff frequency, the 1st and 2nd edge frequency as a function of filling factor for type-1 and type-2 structures respectively. For type-1 structure, since the space averaged dielectric constant becomes lower as the filling factor of plasma rod increases, the cutoff frequency, the 1st and 2nd edge frequencies shift to higher frequency, while for type-2 one in Fig. 8(a), they shift to lower frequency due to the space averaged dielectric constant becomes higher as the filling factor of dielectric rod increases. Figure 7(b) shows $\Delta\omega/\omega_g$ for $TM_{1\text{-}2}$ and $TM_{3\text{-}4}$ in type-1 structure, which almost linearly increase to the filling factor and reach 0.44 and 0.18 at $f = 0.75$, respectively. Instead, the behavior for type-2 plasma PC in Fig. 8(b) is quite different: $\Delta\omega/\omega_g$ for $TM_{1\text{-}2}$ and $TM_{3\text{-}4}$ show maximum values for a given filling factor, and the maximum values for the 1st and 2nd are 0.53 and 0.33 at $f = 0.1$ and $f = 0.25$, respectively.

3.3. Effects of Dielectric Constant on PBG

Figures 9(a) and 10(a) show the cutoff, edge frequencies as a function of dielectric constant for type-1 and type-2 structures respectively. It

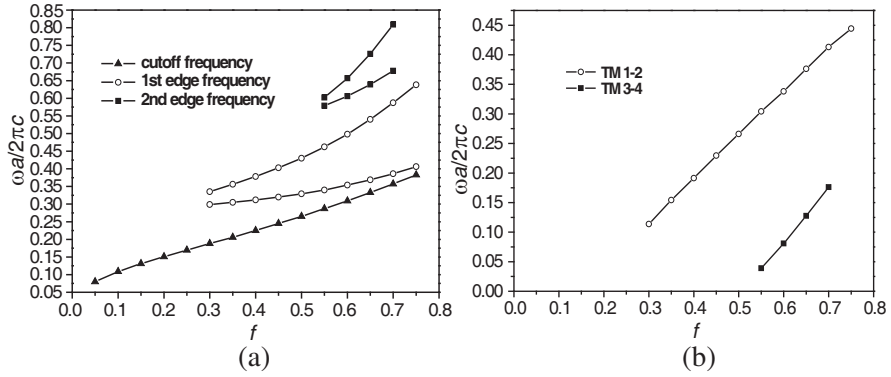

Figure 7. (a) The cutoff frequency, 1st and 2nd PBG edge frequencies, and (b) the 1st and 2nd relative PBG width versus filling factor of plasma rod for type-1 plasma PC with normalized plasma frequency $\omega_p a/2\pi c = 1$ and relative dielectric constant $\varepsilon_b = 6$.

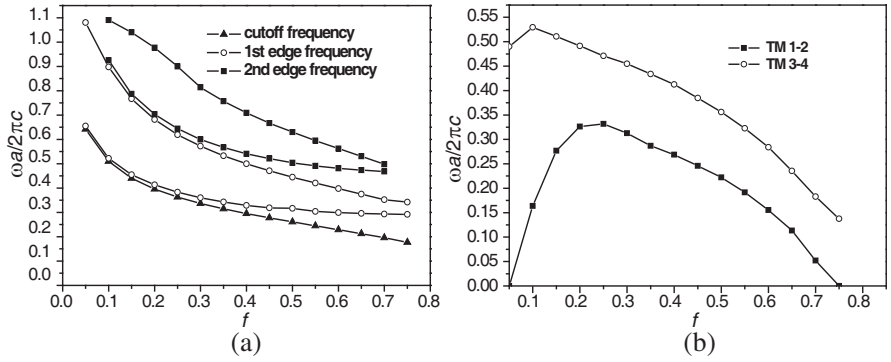

Figure 8. (a) The cutoff frequency, 1st and 2nd PBG edge frequencies, and (b) the 1st and 2nd relative PBG width on the dielectric-filling factor for type-2 plasma PC with normalized plasma frequency $\omega_p a/2\pi c = 1$ and relative dielectric constant of dielectric rod $\varepsilon_a = 6$.

is seen that their cutoff frequency and edge frequencies decrease when dielectric constant increases. This can be explained by the variational principle [25]: the increase of dielectric constant leads to the decrease of the frequency of the modes. This explains the shift of the bands toward the lower frequencies. On the other hand, for the two types of dielectric plasma PC, higher dielectric contrast between the plasma and dielectric will easily lead to large gaps [25, 26]. As seen in Fig. 9(b)

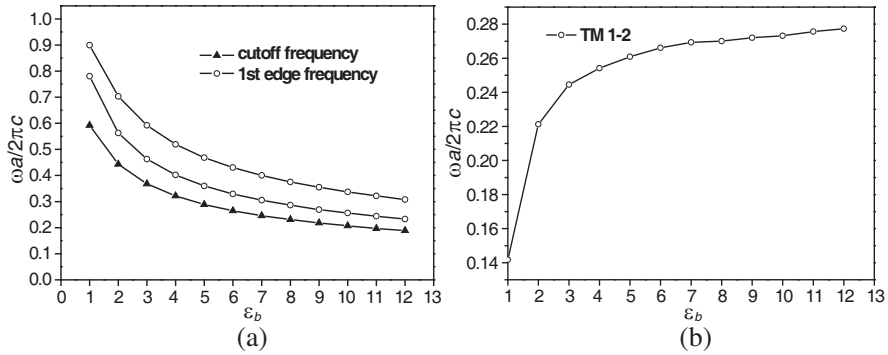

Figure 9. (a) The cutoff frequency, the 1st PBG edge frequencies, and (b) and the 1st relative PBG width versus dielectric constant of background for type-1 plasma PC with normalized plasma frequency $\omega_p a/2\pi c = 1$ and plasma-filling factor $f = 0.5$.

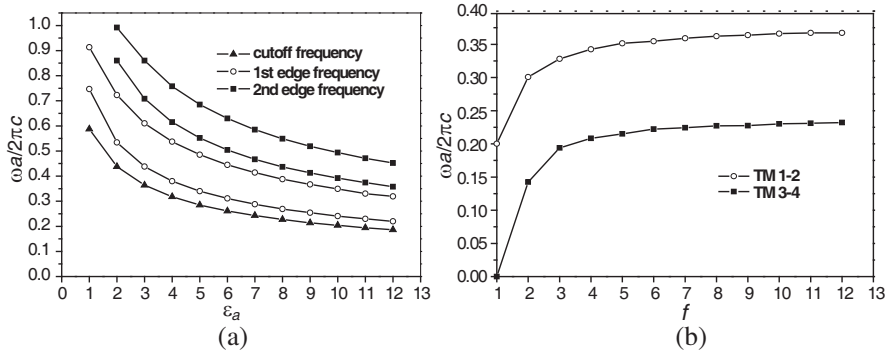

Figure 10. (a) The cutoff frequency, the 1st and 2nd PBG edge frequencies, and (b) the 1st and 2nd relative PBG widths versus dielectric constant of circular rod for type-2 plasma PC with normalized plasma frequency $\omega_p a/2\pi c = 1$ and dielectric-filling factor $f = 0.5$.

and Fig. 10(b), the $\Delta\omega/\omega_g$ increases faster for small relative dielectric constant and tends to stabilize around 0.38 for $TM_{1\text{-}2}$. As for type-2, similar trend exits and the relative PBG widths reach 0.37 and 0.23 at $\varepsilon_b = 12$ for $TM_{1\text{-}2}$ and $TM_{3\text{-}4}$ respectively.

4. CONCLUSIONS

In conclusion, different dispersion characteristics of two types of plasma PC are studied based on modified plane wave method. Results show that the first two photonic band gaps increase when the plasma frequency increases, and the relative PBG width increases faster for small normalized plasma frequency and tends to stabilize. It is worth noting that larger gaps will appear for type-2 plasma PC than that of type-1 when other parameters are the same. It is also seen that the cutoff frequency, the 1st and 2nd edge frequencies shift towards higher frequency when the filling factor of type-1 structure increases. However, they shift toward lower frequencies for type-2 structure, and there are maximum values for 1st and 2nd relative PBG width. When the dielectric constant of type-1 and type-2 plasma PC increases, the cutoff frequency, the 1st and 2nd edge frequencies decrease, while their relative PBG width shift toward large values and become flatten. Therefore, by carefully selecting plasma frequency, filling factor and dielectric constant for the two types of plasma PC, moderate band gap structures can be obtained to meet the needs of application. These results may provide theoretical instructions for designing new PC devices using plasma-dielectric structure.

ACKNOWLEDGMENT

This work is supported by National Key Project for Basic Research of China (Grant No. 2007CB310401) and the National Natural Science Foundation of China (Grant No. 60571020).

REFERENCES

1. Yablonovitch, E., "Inhibited spontaneous emission in solid-state physis and electronics," *Phys. Rev. Lett.*, Vol. 58, 2059–2062, 1987.
2. John, S., "Strong localization of photons in certain disordered dielectric superlattices," *Phys. Rev. Lett.*, Vol. 58, 2486–2489, 1987.
3. Banaei, H. A. and A. Rostami, "A novel proposed for passive all-optical demultiplexer for DWMD systems using 2-D photonic crystals," *J. of Electromagn. Waves and Appl.*, Vol. 22, 471–482, 2008.
4. Manolatou, C., S. G. Johnson, S. Fan, P. R. Villeneuve, H. A. Haus, and J. D. Joannopoulos, "High-density integrated optics," *J. Lightwave Technol.*, Vol. 17, 1682–1692, 1999.

5. Minin, I. V., O. V. Minin, Y. R. Triandaphilov, and V. V. Kotlyar, "Subwavelength diffractive photonic crystal lens," *Progress In Electromagnetics Research B*, Vol. 7, 257–264, 2008.
6. Mizuguchi, J., Y. Tanaka, S. Tamura, and M. Notomi, "Focusing of light in a three-dimensional cubic photonic crystal," *Phys. Rev. B*, Vol. 67, 075109–075117, 2003.
7. Chen, J.-Y., J.-Y. Yeh, L.-W. Chen, Y.-G. Li, and C.-C. Wang, "Design and modeling for enhancement of light extraction in light-emitting diodes with archimedean lattice photonic crystals," *Progress In Electromagnetics Research B*, Vol. 11, 265–279, 2009.
8. Hojo, H. and A. Mase, "Dispersion relation of electromagnetic waves in one dimensional plasma photonic crystals," *J. Plasma Fusion Research*, Vol. 80, No. 2, 89–90, 2004.
9. Liu, S., W. Hong, and N. Yuan, "Finite-difference time-domain analysis of unmagnetized plasma photonic crystals," *International Journal of Infrared and Millimeter Waves*, Vol. 27, No. 3, 403–422, 2006.
10. Sakai, O., T. Sakaguchi, and K. Tachibana, "Verification of a plasma photonic crystal for microwaves of millimeter wavelength range using two-dimensional array of columnar microplasmas," *Appl. Phys. Lett.*, Vol. 87, No. 24, 241505-1-3, 2005.
11. Sakai, O. and K. Tachibana, "Properties of electromagnetic wave propagation emerging in 2-D periodic plasma structures," *IEEE Transactions on Plasma Science*, Vol. 35, No. 5, 1267–1273, 2007.
12. Tachibana, K., Y. Kishimoto, S. Kawai, T. Sakaguchi, and O. Sakai, "Diagnostics of microdischarge-integrated plasma sources for display and material processing," *Plasma Phys. Contr. Fusion*, Vol. 47, A167–A177, 2005.
13. Sakai, O., T. Sakaguchi, and K. Tachibana, "Photonic bands in two-dimensional microplasma arrays. I. Theoretical derivation of band structures of electromagnetic waves," *J. Appl. Phys.*, Vol. 101, No. 7, 073304-1-9, 2007.
14. Sakaguchi, T., O. Sakai, and K. Tachibana, "Photonic bands in two-dimensional microplasma arrays. II. Band gaps observed in millimeter and subterahertz ranges," *J. Appl. Phys.*, Vol. 101, No. 7, 073305-1-7, 2007.
15. Hojo, H., N. Uchida, and A. Mase, "Beaming of millimeter waves from plasma photonic crystal waveguides," *Plasma and Fusion Research: Rapid Communications*, Vol. 1, 021-1-2, 2006.
16. Villa-Villa, F., J. A. Gaspar-Armenta, A. Mendoza-Suárez, "surface modes in one dimensional photonic crystals that include

left handed materials," *J. of Electromagn. Waves and Appl.*, Vol. 21, No. 4, 485–499, 2007.

17. Kuzmiak, V., A. Maradudin, and F. Pincemin, "Photonic band structures of two-dimensional systems containing metallic componets," *Phys. Rev. B*, Vol. 50, No. 23, 16835–16844, 1994.
18. Taflove, A. and S. C. Hagness, *Computational Electrodynamics: The finite-difference time-domain*, 2nd edition, Artech House, Boston, 2000.
19. Moreno, E., D. Erni, and C. Hafner, "Band structure computations of metallic photonic crystals with the multiple multipole method," *Phys. Rev. B*, Vol. 65, No. 15, 155120-1-10, 2002.
20. Srivastava, R., K. B. Thapa, S. Pati, and S. P. Ojha, "Omni-direction reflection in one dimensional photonic crystal," *Progress In Electromagnetics Research B*, Vol. 7, 133–143, 2008
21. Dubey, R. S. and D. K. Gautam, "Development of simulation tools to study optical properties of one-dimentional photonic crystals," *J. of Electromagn. Waves and Appl.*, Vol. 22, 849–860, 2008.
22. Kretschmann, M., "Phase diagrams of surface plasmon polaritonic crystals," *Phys. Rev. B*, Vol. 68, No. 12, 125419-1-5, 2003.
23. *Handbook for CST Microwave Studio V5.1*, 2006.
24. Sakurai, J., *Modern Quantum Mechanics*, Addison-Wesley, New York, 1994.
25. Meade, R. D., A. M. Rappe, K. D. Brommer, and J. D. Joannopoulos, "Nature of the photonic band gap: Some insights from a field analysis," *J. Opt. Soc. Am. B.*, Vol. 10, 328–332, 1993.
26. Joannopoulos, J. D., S. G. Johnson, J. N. Winn, and R. D. Meade, *Photonic Crystals-Molding the Flow of Light*, Princeton University Press, Princeton, 2008.